Original Article

Theabrownin inhibits obesity and non-alcoholic fatty liver disease in mice via serotonin-related signaling pathways and gut-liver axis

Hang-Yu Li [a], Si-Yu Huang [a], Dan-Dan Zhou [a], Ruo-Gu Xiong [a], Min Luo [a], Adila Saimaiti [a], Mu-Ke Han [b], Ren-You Gan [c,*], Hui-Lian Zhu [a], Hua-Bin Li [a,*]

[a] Guangdong Provincial Key Laboratory of Food, Nutrition and Health, Department of Nutrition, School of Public Health, Sun Yat-Sen University, Guangzhou 510080, China
[b] School of Public Health, Capital Medical University, Beijing 100069, China
[c] Research Center for Plants and Human Health, Institute of Urban Agriculture, Chinese Academy of Agricultural Sciences, National Agricultural Science & Technology Center, Chengdu 610213, China

HIGHLIGHTS

- Theabrownin from dark tea markedly prevents and reverses NAFLD and obesity.
- Serotonin-related molecular mechanisms are revealed.
- Gut microbiota is related to serotonin level in liver and visceral adipose tissue.
- Gut microbiota is pivotal for theabrownin to regulate target proteins in liver.
- Interdependent relationships between theabrownin and gut microbiota are revealed.

GRAPHICAL ABSTRACT
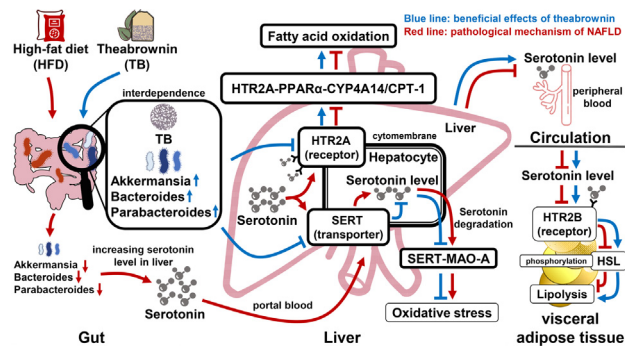
ABSTRACT

Introduction: Non-alcoholic fatty liver disease (NAFLD) with obesity seriously threats public health. Our previous studies showed that dark tea had more potential on regulating lipid metabolism than other teas, and theabrownin (TB) was considered to be a main contributor to the bioactivity of dark tea.
Objectives: This *in vivo* study aims to reveal the effects and molecular mechanisms of TB on NAFLD and obesity, and the role of the gut-liver axis is explored.
Methods: The histopathological examinations, biochemical tests, and nuclear magnetic resonance were applied to evaluate the effects of TB on NAFLD and obesity. The untargeted metabolomics was used to find the key molecule for further exploration of molecular mechanisms. The 16S rRNA gene sequencing was used to assess the changes in gut microbiota. The antibiotic cocktail and fecal microbiota transplant were used to clarify the role of gut microbiota.
Results: TB markedly reduced body weight gain (67.01%), body fat rate (62.81%), and hepatic TG level (51.35%) in the preventive experiment. Especially, TB decreased body weight (32.16%), body fat rate (42.56%), and hepatic TG level (42.86%) in the therapeutic experiment. The mechanisms of action could be the improvement of fatty acid oxidation, lipolysis, and oxidative stress via the regulation of serotonin-related signaling pathways. Also, TB increased the abundance of serotonin-related gut microbiota, such as *Akkermansia*, *Bacteroides* and *Parabacteroides*. Antibiotics-induced gut bacterial dysbiosis disrupted the regulation of TB on serotonin-related signaling pathways in liver, whereas the beneficial regulation of

TB on target proteins was regained with the restoration of gut microbiota.

Conclusion: We find that TB has markedly preventive and therapeutic effects on NAFLD and obesity by regulating serotonin level and related signaling pathways through gut microbiota. Furthermore, gut microbiota and TB co-contribute to alleviating NAFLD and obesity. TB could be a promising medicine for NAFLD and obesity.

Introduction

Non-alcoholic fatty liver disease (NAFLD) is a serious public health problem in the world [1]. In general, the global prevalence of NAFLD is around 25 % of the adult population, and it is a leading cause of cirrhosis and hepatocellular carcinoma [2]. It has been reported that 80 % of people with obesity have different degrees of NAFLD, and weight loss is beneficial to alleviating NAFLD [2–4]. Therefore, the prevention and treatment of NAFLD should consider both the alleviation of hepatic steatosis and the promotion of weight loss [5].

Pathologically, the deposition of triglyceride (TG) as lipid droplets in the cytoplasm of hepatocytes is the fundamental feature of NAFLD, and the dysbiosis of gut microbiota plays an important role in the development of hepatic steatosis [6,7]. For example, the abundance of *Bifidobacterium* was decreased in patient with NAFLD and obesity, and the reduced ratio of *Bacteroidetes* to *Firmicutes* could be a risk factor of the progression of NAFLD [8,9]. Moreover, the accumulation of visceral white adipose tissue and oxidative stress are also involved in the pathogenesis of NAFLD [10]. Serotonin is a bioamine converted from tryptophan, and the conversion is mainly proceeded by the enterochromaffin cells of gut [11]. Additionally, the peripheral serotonin derived from enterochromaffin cells could be an endocrine regulator for lipid metabolism [12]. Further studies in pathological mechanisms showed that serotonin could interact with serotonin receptor 2A (HTR2A) and serotonin transporter (SERT) to induce hepatic steatosis and oxidative stress in liver, on the other hand, serotonin could activate serotonin receptor 2B (HTR2B) to promote lipolysis in visceral white adipose tissue [13,14]. Although gut microbiota has been well proved to be involved in the synthesis of peripheral serotonin [15], whether the regulation of gut microbiota could affect the content and function of serotonin in liver is unknown.

In our previous study, we summarized that the intake of plant-based foods (like tea), as well as their bioactive components, might be beneficial to attenuating NAFLD and body weight gain [16]. Tea (*Camellia sinensis*) is a healthy beverage, and it is divided into different categories according to different fermentation degrees, such as green tea (unfermented), black tea (completely fermented), and dark tea (post-fermented) [17–19]. Our previous study showed that dark tea was beneficial to gut microbial homeostasis, and it had more potential on regulating lipid metabolism than other teas, which confirmed similar findings from other researchers [18,20–22]. Dark tea is produced by the post-fermentation of fresh *Camellia sinensis* leaves, which gives it the highest content of theabrownin (TB) among all categories of teas [23]. TB is considered to be the main contributor to the difference in bioactivity between dark tea and other teas [19]. So, it is reasonable to hypothesize that TB could effectively promote lipid clearance and might be a medicine for NAFLD and obesity.

In this study, we evaluated the preventive and therapeutic effects of TB on NAFLD and obesity via histopathological examination, biochemical test, and nuclear magnetic resonance. Then, the untargeted metabolomics and further quantitative assay were used to discover the key molecule linked to NAFLD and obesity. Following these clues, the molecular mechanisms were further verified.

Moreover, the 16S rRNA gene sequencing was used to assess the changes in gut microbiota. Besides, the antibiotic cocktail was used to deplete gut microbiota for clarifying the role of gut microbiota in regulating molecular mechanisms. Additionally, fecal microbiota transplant was used to identify whether TB or gut microbiota was the key factor in action.

Materials and Methods

Ethics statement

All experiments in this study were conducted according to the national legislation and the guidelines of the laboratory animal center at Sun Yat-Sen University (Guangzhou, China). All experimental procedures were approved by the Ethics Committee in the School of Public Health, Sun Yat-Sen University (No. 2019–002).

Animal experiment design

The 4-week-old specific-pathogen-free (SPF) C57BL/6J male mice were purchased from the Guangdong medical laboratory animal center (Guangzhou, China). All mice were maintained in the SPF animal facility under controlled conditions (22 to 24 °C room temperature, 50 % to 60 % relative humidity, and a 12-hour light/-dark cycle). The C57BL/6J mice were fed either a control diet (CD) (D12450J, Research Diet, USA) or a high-fat diet (HFD) (D12492, Research Diet, USA) (Table S1). Besides, a part of C57BL/6J mice received the antibiotic cocktail to prepare the antibiotics-sterilized mice for the antibiotic interference experiment and fecal microbiota transplant experiment [24]. The antibiotic cocktail contained ampicillin (A9518, Sigma Aldrich, Germany), metronidazole (M3761, Sigma Aldrich, Germany), neomycin (N6386, Sigma Aldrich, Germany), and vancomycin (V2002, Sigma Aldrich, Germany). The antibiotic cocktail was added to drinking water, and their concentrations were 1.0 mg/mL of ampicillin, 1.0 mg/mL of metronidazole, 1.0 mg/mL of neomycin, and 0.5 mg/mL of vancomycin, respectively. The drinking water containing antibiotic cocktail was provided to mice for two weeks, meanwhile, an extra 300 μL of the antibiotic cocktail was intragastrically provided during the first five days [25]. According to the previous studies and the difference in body surface area in different animal models, TB (Yunnan Tearevo Biotechnology, China) was dissolved in sterilized water (250 mg/mL) and intragastrically provided to mice (2,300 mg/kg/day) [26,27]. The body weight and food intake were recorded. The blood, feces, liver, and visceral white adipose tissue were collected at the end of the experiments after being euthanized. Here, we briefly described the design of the four main experiments.

The preventive and therapeutic experiments

The 14-week preventive experiment was designed to explore the preventive effect and the molecular mechanisms of TB on hepatic steatosis and fat accumulation. Also, the changes in gut microbiota were evaluated. Forty C57BL/6J mice were randomly divided

into four groups: blank control (CD group), TB control (CD + TB group), NAFLD with obesity (HFD group), and TB intervention (HFD + TB group). Besides, the feces of mice in the HFD and HFD + TB groups were collected during the 7th to 14th week for fecal microbiota transplant experiment.

The 28-week therapeutic experiment was designed to evaluate the therapeutic effect of TB on NAFLD and obesity. Meanwhile, the changes in oxidative stress were assessed. For the first fourteen weeks, ten C57BL/6J mice were fed a HFD to induce NAFLD and obesity. For the next fourteen weeks, the model mice were randomly divided into two groups. A group of mice continued to receive HFD alone (HFD group). Another group of mice received a HFD and TB (HFD + TB group).

The antibiotic interference and fecal microbiota transplant experiments

The antibiotic interference experiment was designed to evaluate the importance of gut microbiota for TB in regulating target proteins in liver. Fifteen C57BL/6J mice were randomly divided into three groups, and all mice were fed a HFD. A group of mice received TB for seven weeks (TB group). Another group of mice received TB for seven weeks and the extra antibiotic cocktail was supplied within the last two weeks (TB + AB group). The last group of mice firstly received an antibiotic cocktail to deplete the original gut microbiota, after that, the sterilized mice were transplanted with fecal microbiota and simultaneously received TB (TB + FMT group). The fecal microbiota was derived from the TB group.

The fecal microbiota transplant experiment was designed to identify whether TB or gut microbiota was the key factor in action in this study. The fecal microbiota was derived from the HFD and HFD + TB groups in the 14-week preventive experiment. Thirty antibiotics-sterilized mice were fed a HFD and randomly divided into three groups. A group of mice was transplanted with fecal microbiota derived from the HFD group for seven weeks (Model FMT group). A group of mice was transplanted with fecal microbiota derived from the HFD + TB group for seven weeks (TB FMT group). The last group of mice were transplanted with fecal microbiota derived from the HFD + TB group and simultaneously received TB (TB FMT + TB group).

The procedure of fecal microbiota transplant referred to a previous study with slight modifications [28]. Briefly, the C57BL/6J mice in the HFD and TB groups in the 14-week preventive experiment were selected as donor mice for feces. On the day of the transplantation, the 200 mg of fresh feces were dispersed in 1 mL of 37 ℃ sterilized phosphate-buffered saline (PBS) and fully blended [29]. Next, the mixture was centrifuged at 1,500 rpm/min for 5 min to isolate the supernatant. Further, antibiotics-sterilized mice immediately received 300 μL of the supernatant by gavage once a day for the first five days and repeated gavage once a week for the rest of seven weeks to reinforce the effects of fecal microbiota transplant [29–31]. Besides, the extra supplement of the antibiotic cocktail was terminated during the fecal microbiota transplant period.

Liver histopathology, ROS fluorescence staining, and nuclear magnetic resonance

The liver pathological examination included hematoxylin and eosin (H&E) staining, Oil red O staining, and reactive oxygen species (ROS) fluorescence staining, and the procedure referred to previous studies with slight modifications [32,33]. The H&E and Oil red O staining were performed in a routine histopathological examination. For H&E staining, the liver tissues were fixed with 4 % paraformaldehyde and embedded with paraffin [32]. For Oil red O staining, the liver tissues were frozen in optimal cutting temperature compound (OCT 4583, SAKURA, Japan) [32]. Besides, a

part of OCT-frozen liver tissue was used to evaluate the oxidative stress via ROS assay kit by using 2,7-dichlorofluorescein diacetate (DCFH-DA) as the fluorescent probe (S0033S, Beyotime Technology, China) [33]. Furthermore, the fluorescence images were obtained via the automated acquisition system (TissueFAXS Plus, TissueGnostics GmbH, Austria) [34]. Additionally, the body fat rate and adipose tissue distribution of mice were analyzed via the nuclear magnetic resonance analyzer (QMR23-040H-I, Suzhou Niumag Analytical Instrument Corporation, China) [35,36]. The original results of nuclear magnetic resonance without pseudo color are provided in Fig. S1.

Biochemical and oxidative stress indexes of liver and serum

Liver tissue was homogenized in cold saline (1:10, m/v) and centrifuged twice at 3,000 rpm/min for 10 min, and the supernatant was collected. Then, the supernatant was used to measure the hepatic levels of TG and total cholesterol (TC) via commercial kits (A110-1–1 and A111-1–1, Nanjing Jiancheng Bioengineering Institute, China) [37]. Moreover, the serum levels of TG, TC, high-density lipoprotein cholesterol (HDL-C), low-density lipoprotein cholesterol (LDL-C), alanine aminotransferase (ALT), and aspartate aminotransferase (AST) were evaluated by the automatic biochemical analyzer (Chemray 800, Rayto, China) according to the manufacturer's protocol [33,37]. Furthermore, the hepatic malondialdehyde (MDA), superoxide dismutase (SOD), and catalase (CAT) were measured by commercial kits (A003-1–2, A001-3–2, and A007-1–1, Nanjing Jiancheng Bioengineering Institute, China) [38].

Untargeted metabolomics study

The procedure of untargeted metabolomics study referred to previous literature [39]. The serum samples were thawed at 4 ℃, then the 100 μL of each sample was transferred into 2 mL centrifuge tubes. Next, the 400 μL of methanol (-20 ℃) was added to each tube and vortexed for 60 s. The mixture system was centrifuged at 12,000 rpm/min for 10 min under 4 ℃ and the supernatant was transferred into another 2 mL centrifuge tube. Further, the supernatants were concentrated and dried in a vacuum. Then, the dry samples were dissolved with 150 μL of 80 % methanol solution containing 2-chlorobenzalanine (4 ppm). After that, the supernatant was filtered by a 0.22 μm membrane to prepare samples for liquid chromatography-mass spectrometry (LC-MS). Besides, an extra 20 μL of each sample was taken to conduct quality control for monitoring the deviations in the process of sample pretreatment and the whole measuring system.

Chromatographic separation was accomplished in a Thermo Vanquish system equipped with an ACQUITY UPLC HSS T3 (150 × 2.1 mm, 1.8 μm, Waters, USA) column maintained at 40 ℃. The temperature of the autosampler was 8 ℃. For the positive model, the gradient elution of analytes was carried out with 0.1 % formic acid in water (A2) and 0.1 % formic acid in acetonitrile (B2). For the negative model, the gradient elution of analytes was carried out with 5 mM ammonium formate in water (A3) and pure acetonitrile (B3). After equilibrating, the 2 μL of each sample was injected into the system to conduct gradient elution at a flow rate of 0.25 mL/min. An increasing linear gradient of solvent B2 or B3 was used as follows: 0 ∼ 1 min, 2 % B2 or B3; 1 ∼ 9 min, 2 %∼ 50 % B2 or B3; 9 ∼ 12 min, 50 %∼98 % B2 or B3; 12 ∼ 13.5 min, 98 % B2 or B3; 13.5 ∼ 14 min, 98 %∼2% B2 or B3; 14 ∼ 20 min, 2 % B2-positive model or 14 ∼ 17 min, 2 % B3-negative model.

The electrospray ionization tandem mass spectrometry experiments (ESI-MSn) proceeded on the Thermo Q Exactive mass spectrometer with the spray voltage of 3.5 kV and −2.5 kV in positive and negative modes, respectively. The sheath gas and auxiliary

gas were set at 30 and 10 arbitrary units, respectively. The capillary temperature was 325 °C. The mass resolution of the analyzer was set at 70,000 and proceeded full scan (the mass range of m/z from 81 to 1,000). The data-dependent acquisition MS-MS experiments were performed with higher energy collision-induced dissociation (HCD) scan. The normalized collision energy was 30 eV. The dynamic exclusion was implemented to remove unnecessary information in MS-MS spectra. By restricting the relative molecular mass to < 30 ppm error, the exact molecular weight of metabolites would be determined. Further information was obtained from databases such as the human metabolome database (HMDB), METLIN, MassBank, LipidMaps, mzCloud, as well as the self-developed metabolomic database of PANOMIX Biomedical Tech (Suzhou, China).

Enzyme-linked immunosorbent assay (ELISA)

The levels of serotonin in liver and visceral white adipose tissue were evaluated by ELISA kit (CSB-E08365m, CUSABIO, China) [40]. Briefly, 100 mg liver or visceral white adipose tissue was rinsed and homogenized in 1 mL of PBS. Next, the homogenates suffered two freeze–thaw cycles to break the cell membranes, and then the mixture was centrifuged for 5 min at 7,300 rpm/min. The supernatants were collected and further used to determine the optical density (OD) with a microplate reader at 450 nm, then the level of serotonin was calculated based on a standard curve.

Western blot analysis

The western blot analysis was performed as the previous description with slight modifications [14,41]. The details of sample preparing were exhibited in supplementary text. Briefly, the liver and visceral white adipose tissue were directly lysed in RIPA buffer containing PMSF, and the supernatants were used to detect HTR2A, peroxisome proliferator-activated receptor α (PPARα), cytochrome P450 family of 4A14 (CYP4A14), SERT, HTR2B, hormone-sensitive lipase (HSL), and the phosphorylation of HSL (p-HSL). Besides, hepatic mitochondrial proteins were firstly isolated and then lysed in RIPA buffer for detecting monoamine oxidase A (MAO-A) and carnitine palmitoyltransferase-1 (CPT-1). Next, the aliquots of 40 μg denatured proteins were separated by 10 % sodium dodecyl sulfate–polyacrylamide gel electrophoresis (SDS-PAGE). The voltage-dependent anion-selective channel protein 1 (VDAC1) was chosen as the loading control for MAO-A and CPT-1, while β-actin was chosen as the loading control for the rest of the target proteins. The dilutions of primary and secondary antibodies were exhibited in supplementary text.

Bacterial DNA extraction and 16S rRNA gene sequencing

The bacterial DNA extraction and 16S rRNA sequencing were performed as the previous description with minor modifications [42]. The relative details were exhibited in supplementary text. Briefly, total microbial genomic DNA samples were extracted by using the OMEGA Soil DNA Kit (M5635-02, Omega Bio-Tek, USA) with mechanical lysis via bead grinding. The polymerase chain reaction (PCR) amplification of the bacterial 16S rRNA gene V3-V4 regions was performed using the forward primer 338F (5′-ACTCCTACGGGAGGCAGCA-3′) and the reverse primer 806R (5′-TCGGACTACHVGGGTWTCTAAT-3′). The PCR amplicons were purified with Vazyme VAHTSTM DNA Clean Beads (Vazyme, China) and quantified using the Quant-iT PicoGreen dsDNA Assay Kit (Invitrogen, USA). After the individual quantification step, amplicons were pooled in equal amounts, and pair-end 2 × 250 bp sequencing was performed using the Illumina TruSeq Nano DNA LT Library Prep at Suzhou PANOMIX Biomedical Tech (Suzhou, China).

Statistical and bioinformatic analysis

The differential analysis of conventional indexes was conducted with SPSS software (version 26.0, IBM, USA), and the procedure referred to a previous study with slight modifications [43]. Based on the results of the normality test, the data were represented as mean with standard deviation (SD) or median with interquartile range. Moreover, the Student's t-test and the analysis of variance (ANOVA) were used when the datasets showed normal distribution and homoscedasticity, otherwise, the Mann-Whitney U test and the Kruskal-Wallis test would be used. The P-value < 0.05 was deemed as a significant difference. All bar plots in our study were generated by GraphPad Prism (version 9.0.0, GraphPad Software, USA).

The analysis of data in the untargeted metabolomics study referred to previous studies with slight modifications [39,44]. The details of data processing were exhibited in supplementary text. Briefly, the Proteowizard (Proteowizard software, USA) and the R package XCMS were used to process data. The information on quality assurance and quality control is presented in Fig. S2 and S3. The partial least squares discriminant analysis (PLS-DA) was used to identify the differences of metabolites among groups, and the orthogonal partial least squares discriminant analysis (OPLS-DA) was used to maximize the discrimination and generate the "variable importance for the projection" (VIP value). To screen the differential metabolites, the inclusion criteria were set as follows: the univariate statistical analysis with the P-value < 0.05 and the VIP value greater than 1. The metabolic pathway enrichment analysis of differential metabolites was performed using the Kyoto encyclopedia of genes and genomes (KEGG) databases.

Microbiome bioinformatics was performed by "the quantitative insights into microbial ecology 2" (QIIME2) and R packages (version 3.2.0), and the procedure referred to the official tutorials and a previous study with slight modifications [45]. The details of data processing were exhibited in supplementary text. Briefly, the taxonomic analysis of non-singleton amplicon sequence variants (ASVs) based on the Greengenes database (Release 13.8) were used to calculate the α-diversity and β-diversity of gut microbiota. Meanwhile, the amplicon sequences of each sample were rarefied to equal sequences for normalization (43,962 sequences for the 14-week preventive experiment and 34,758 sequences for the antibiotic interference experiment). The α-diversity metrics (including Chao1 index, observed species richness, Shannon index, Simpson's index of diversity (also known as "1-D"), and Pielou's evenness) were used to compare the richness and evenness. The β-diversity was analyzed by the principal coordinate analysis (PCoA) with the Bray-Curtis and UniFrac distance to investigate the structural variation of gut microbial communities across groups. Furthermore, the significant difference in microbiota structure among different groups was assessed by the permutational multivariate analysis of variance (PERMANOVA). The linear discriminant analysis effect size (LEfSe) and the random forests analyses were used to identify differential taxa between groups. The changes in gut bacterial function were predicted by the "phylogenetic investigation of communities by reconstruction of unobserved states" (PICRUSt2) and the KEGG databases.

Results

TB possesses preventive and therapeutic effects on NAFLD and obesity

In the 14-week preventive experiment, HFD induced the typical pathological features of NAFLD with hepatic steatosis, body fat accumulation, and a significant increase in body weight (Fig. 1A-C, and Fig. S1). On the other hand, TB significantly prevented hep-
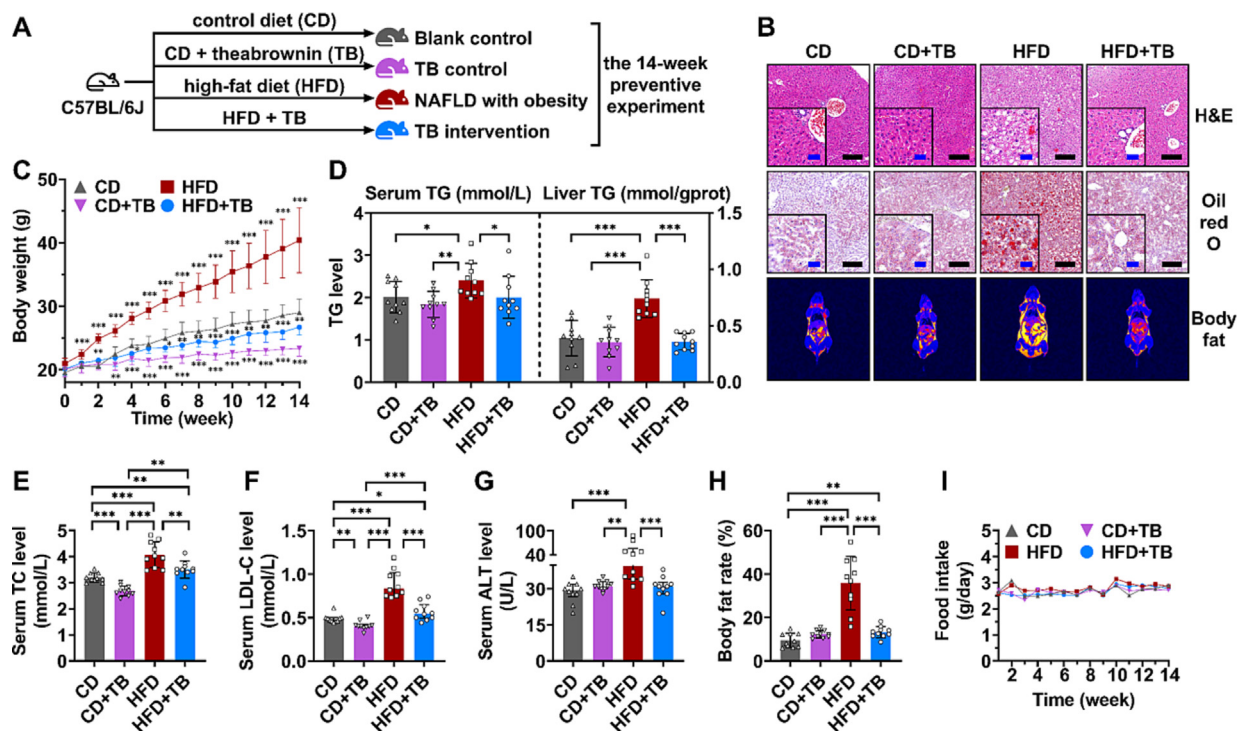
Fig. 1. The preventive effect of TB on NAFLD and obesity. (A) The simplified flow chart. **(B)** Hepatic H&E and Oil red O staining (black scale bar = 200 μm and blue scale bar = 50 μm), and body fat distribution scanned by NMR (the adipose tissue is highlighted. **(C)** The changes in body weight (the *P*-values were calculated by comparing different groups with CD group). **(D)** The level of TG in serum and liver. **(E)** The level of TC in serum. **(F)** The level of LDL-C in serum. **(G)** The level of ALT in serum. **(H)** Body fat rate. **(I)** The average daily food intake of a mouse per week. Data are shown as mean with SD or median with interquartile range, n = 10. Data were analyzed by either ANOVA or Kruskal-Wallis test. *P*-value < 0.05, **P*-value < 0.01, ***P*-value < 0.001. The symbols of triangle, inverted triangle, square and circle on the bars represent the samples of CD group, CD + TB group, HFD group, and HFD + TB group, respectively. Abbreviation: ALT, alanine aminotransferase; ANOVA, analysis of variance; CD, control diet; H&E, hematoxylin and eosin; LDL-C, low-density lipoprotein cholesterol; HFD, high-fat diet; NMR, nuclear magnetic resonance; TB, theabrownin; TC, total cholesterol; TG, triglyceride; SD, standard deviation.

atic steatosis, body fat accumulation, and body weight gain (Fig. 1-A-C, and Fig. S1). For example, body weight gain in HFD + TB group was 67.01 % lower than that in HFD group (*P*-value < 0.001). Moreover, TB decreased the level of TG in serum and liver and reduced the serum levels of TC, LDL-C, and ALT (Fig. 1D-G). For example, hepatic TG level in HFD + TB group was 51.35 % lower than that in HFD group (*P*-value < 0.001). Furthermore, TB prevented the increase in body fat rate without affecting the appetite of mice, and body fat rate in HFD + TB group was 62.81 % lower than that in HFD group (*P*-value < 0.001) (Fig. 1H, I). To further evaluate the therapeutic effect of TB on NAFLD and obesity, we conducted the 28-week therapeutic experiment (Fig. 2A). After extending the experimental period, TB showed the potential to be a medicine for NAFLD and obesity by reversing hepatic steatosis, body fat accumulation and promoting body weight loss (Fig. 2B-D). For example, body weight in HFD + TB group was 32.16 % lower than that in HFD group (*P*-value < 0.001), meanwhile, body fat rate in HFD + TB group was 42.56 % lower than that in HFD group (*P*-value < 0.001). Besides, TB improved the levels of TG, TC, HDL-C, LDL-C, ALT and AST in serum and liver during the 28-week therapeutic experiment (Fig. 2E-H). For example, hepatic TG level in HFD + TB group was 42.86 % lower than that in HFD group (*P*-value < 0.05). Additionally, we assessed the changes in hepatic oxidative stress during the 28-week therapeutic experiment. TB reduced the relative level of ROS and the content of MDA but increased the activities of SOD and CAT in liver (Fig. 2I-K).

In short, TB possessed preventive and therapeutic effects on NAFLD and obesity by alleviating hepatic steatosis, body fat accumulation, body weight gain, dyslipidemia and oxidative stress.

TB changes the level of serotonin in liver, blood circulation, and visceral white adipose tissue

To discover the key molecule for TB to alleviate NAFLD and obesity, we conducted an untargeted metabolomics study in the 14-week preventive experiment. The untargeted metabolomics study identified 1,691 metabolites in serum, among which 243 metabolites showed significant differences among groups (the data are exhibited in the MetaboLights repository: MTBLS4879). Particularly, TB intervention significantly affected the levels of metabolites involved in tryptophan metabolism (Fig. 3A). Moreover, the changes in serotonin level caught our attention after comparing the fold change of metabolites among the blank control (CD group), TB control (CD + TB group), NAFLD with obesity (HFD group), and TB intervention (HFD + TB group). To be specific, the HFD group had a lower level of serotonin in serum compared with the CD group (Fig. 3B). Furthermore, the CD + TB and HFD + TB groups had a higher level of serotonin in serum compared with the CD and HFD groups (Fig. 3B). These findings indicated that serotonin could be a pivotal molecule responded to TB intervention. Subsequently, we quantified the level of serotonin in liver by ELISA. In the 14-week preventive experiment, the HFD + TB group showed a significantly decreased level of serotonin in liver compared with the HFD group (Fig. 3C). Because the accumulation of visceral adipose white tissue is one of the characterized features of NAFLD and obesity, we further measured and revealed that TB significantly increased the level of serotonin in visceral white adipose tissue (Fig. 3D).
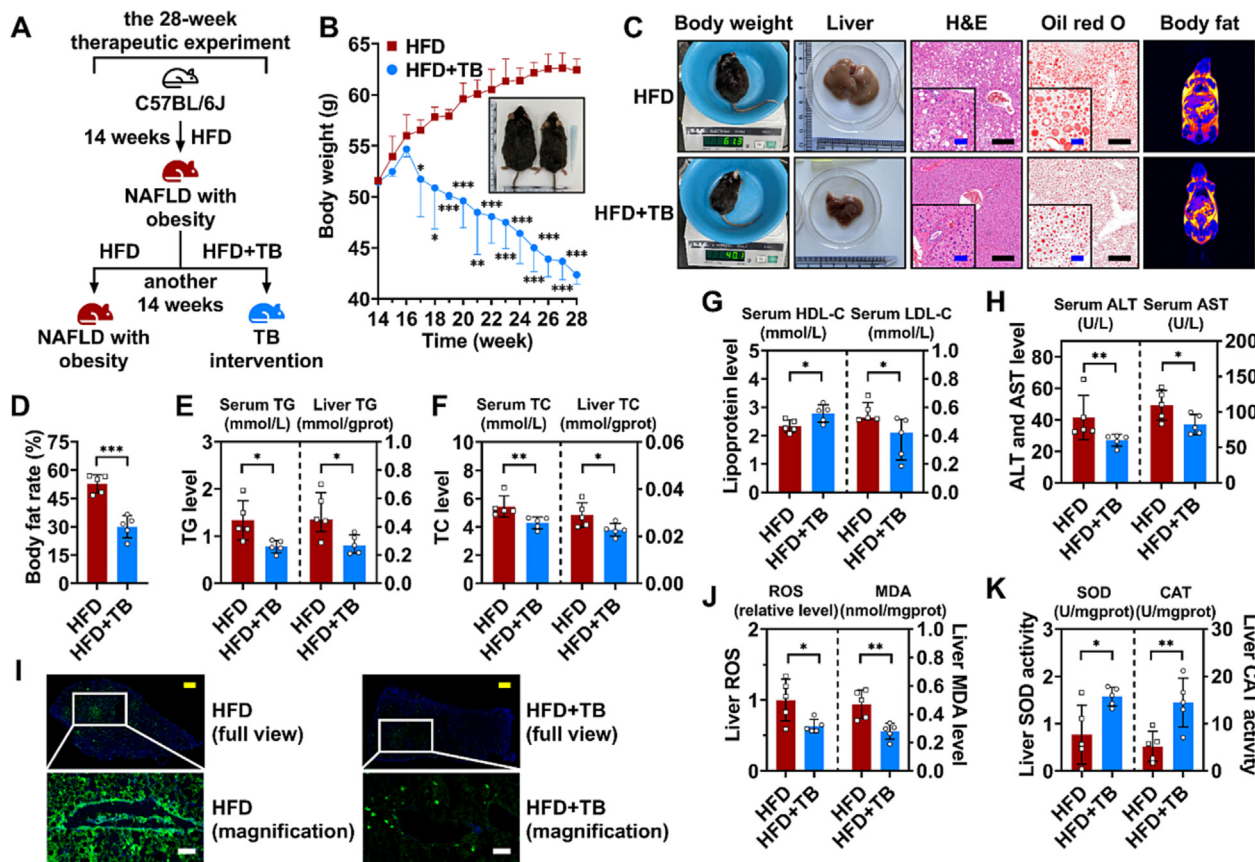
Fig. 2. The therapeutic effect of TB on NAFLD and obesity. (A) The simplified flow chart. **(B)** The changes in body weight. **(C)** The photographic records, hepatic H&E and Oil red O staining (black scale bar = 200 μm and blue scale bar = 50 μm), and body fat distribution scanned by NMR (the adipose tissue is highlighted). **(D)** Body fat rate. **(E)** The level of TG in serum and liver. **(F)** The level of TC in serum and liver. **(G)** The levels of HDL-C and LDL-C in serum. **(H)** The levels of ALT and AST in serum. **(I)** The ROS fluorescence images of liver (bright green area is ROS fluorescence, yellow scale bar = 1,000 μm and white scale bar = 20 μm). **(J)** The relative ROS fluorescence intensity and MDA level in liver. **(K)** The activities of SOD and CAT in liver. Data are shown as mean with SD or median with interquartile range, n = 5. Data were analyzed by either two-tailed Student's *t*-test or Mann-Whitney *U* test. *P-value < 0.05, **P-value < 0.01, ***P-value < 0.001. The symbols of square and circle on the bars represent the samples of HFD group and HFD + TB group, respectively. Abbreviation: ALT, alanine aminotransferase; AST, aspartate aminotransferase; CAT, catalase; HDL-C, high-density lipoprotein cholesterol; H&E, hematoxylin and eosin; HFD, high-fat diet; LDL-C, low-density lipoprotein cholesterol; MDA, malonaldehyde; NMR, nuclear magnetic resonance; ROS, reactive oxygen species; SD, standard deviation; SOD, superoxide dismutase; TB, theabrownin; TC, total cholesterol; TG, triglyceride.

In short, TB decreased the level of serotonin in liver while increased the level of serotonin in blood circulation and visceral white adipose tissue.

TB alleviates NAFLD and obesity by regulating serotonin-related signaling pathways

We further explored the molecular mechanisms of TB to alleviate NAFLD and obesity. The overexpression of HTR2A had been considered as a risk factor for hepatic steatosis [13]. Consistently with the decreased level of serotonin in liver, the HFD + TB group had a decreased expression of HTR2A in liver compared with the HFD group in the 14-week preventive experiment (Fig. 3C, and Fig. 4A, B). Subsequently, TB increased the expressions of downstream molecules negatively regulated by HTR2A, including PPARα and CYP4A14 (Fig. 4A, B). The regulation of TB on the HTR2A-PPARα-CYP4A14 signaling pathway could promote fatty acid oxidation in liver and then alleviate NAFLD. Besides, serotonin had been recognized as a beneficial factor to enhance lipolysis via HTR2B and HSL in white adipocytes [14]. Consistently with the increased level of serotonin in visceral white adipose tissue, TB significantly promoted lipolysis by activating HTR2B-mediated phosphorylation of HSL in the 14-week preventive experiment (Fig. 4C, D). Further, the molecular mechanism related to oxidative stress was explored using hepatic tissue and mitochondria collected from

the 28-week therapeutic experiment. As we expected, TB mitigated oxidative stress by decreasing the expressions of SERT and MAO-A (a key protein to degrade serotonin and then provoke oxidative stress) (Fig. 4E, F). Besides, TB increased the expression of CPT-1 (a downstream protein of PPARα) in the 28-week therapeutic experiment, which was beneficial to TG clearance (Fig. 4E, F).

In short, TB promoted fatty acid oxidation to alleviate hepatic steatosis by regulating the HTR2A-PPARα-CYP4A14/CPT-1 signaling pathway in liver. Moreover, TB promoted lipolysis to reduce body fat accumulation by activating the HTR2B-HSL signaling pathway in visceral white adipose tissue. Furthermore, TB mitigated oxidative stress by inhibiting the SERT-MAO-A signaling pathway in liver.

Gut microbiota is correlated to serotonin distribution

To evaluate the effect of TB on gut microbiota, we conducted the 16S rRNA gene sequencing using feces collected from the 14-week preventive experiment. The data of the 16S rRNA gene sequencing in this study are deposited in the NCBI Sequence Read Archive (SRP) repository: PRJNA839260. Firstly, TB increased the richness and evenness of gut microbiota. The α-diversity indexes (such as Chao1 index, observed species richness, Shannon index, Simpson's index of diversity, and Pielou's evenness) were higher in the CD + TB and HFD + TB groups than those in the CD and HFD groups
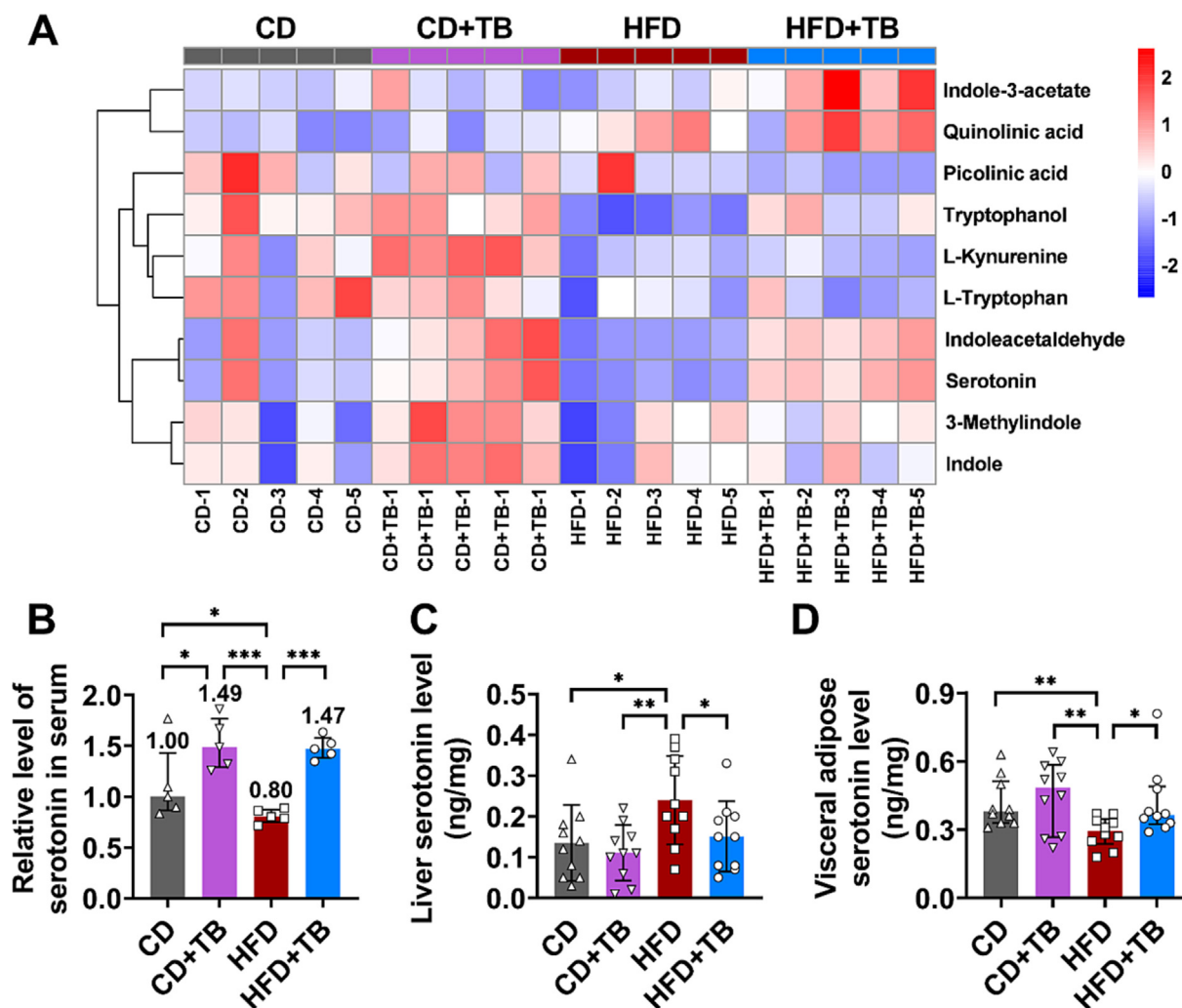
Fig. 3. The changes in serotonin distribution from TB intervention. (A) Heatmap for the representative metabolites involved in tryptophan metabolism according to the untargeted metabolomics study. **(B)** The relative level of serotonin in serum according to the untargeted metabolomics study. **(C)** The evaluation of serotonin level in liver by ELISA. **(D)** The evaluation of serotonin level in visceral white adipose tissue by ELISA. Data are shown as mean with SD or median with interquartile range, n = 5 or 10. Data were analyzed by either ANOVA or Kruskal-Wallis test. $*P < 0.05$, $**P$-value < 0.01, $***P$-value < 0.001. The symbols of triangle, inverted triangle, square and circle on the bars represent the samples of CD group, CD + TB group, HFD group, and HFD + TB group, respectively. Abbreviation: ANOVA, analysis of variance; CD, control diet; ELISA, enzyme-linked immunosorbent assay; HFD, high-fat diet; SD, standard deviation; TB, theabrownin.

(Fig. 5A-E). Then, the gut microbial community across groups was significant differences according to the evaluation of β-diversity (Fig. 5F, G).

With the help of the LEfSe and the random forests analysis, the representative gut bacterial genera were identified, such as *Akkermansia*, *Bacteroides* and *Parabacteroides*. To be specific, the gut bacterial genera *Akkermansia*, *Bacteroides* and *Parabacteroides* significantly responded to TB intervention, and they were key contributors to the β-diversity across groups (Fig. 5H and Fig. S4). Moreover, the CD + TB and HFD + TB groups had significantly higher abundances of *Akkermansia*, *Bacteroides* and *Parabacteroides* than those in the CD and HFD groups (Fig. 5I). The changes in gut bacterial composition often led to the changes in gut bacterial function [46]. Further network and predictive analyses showed that gut bacterial genera *Akkermansia*, *Bacteroides* and *Parabacteroides* were connected to other genera and formed as specific modules, which played a vital role in the metabolic function of gut microbiota (Fig. S5). More importantly, the multi-omics analysis based on the untargeted metabolomics and the 16S rRNA gene sequencing showed that the serotonin in blood circulation was positively correlated to *Akkermansia* (correlation coefficient

$(r) = 0.647$), *Bacteroides* ($r = 0.612$), and *Parabacteroides* ($r = 0.640$) (Fig. 5J). Whereas, the serotonin in liver was negatively correlated to *Akkermansia* ($r = -0.808$), *Bacteroides* ($r = -0.684$) and *Parabacteroides* ($r = -0.689$) (Fig. 5J). Besides, the serotonin in visceral white adipose tissue was positively correlated to *Akkermansia* ($r = 0.697$), *Bacteroides* ($r = 0.606$) and *Parabacteroides* ($r = 0.698$) (Fig. 5J).

In a word, TB increased the abundances of gut bacterial genera *Akkermansia*, *Bacteroides* and *Parabacteroides*. These genera were negatively correlated to the level of serotonin in liver while positively correlated to the level of serotonin in blood circulation and visceral white adipose tissue.

Gut microbiota is pivotal for TB to regulate serotonin-related signaling pathways in liver

To verify the importance of gut microbiota for TB to regulate serotonin-related signaling pathways in liver, we designed the antibiotic interference experiment referred to a previous study with minor modifications [47]. The simplified flow chart of the antibiotic interference experiment is exhibited in Fig. 6A. The extra
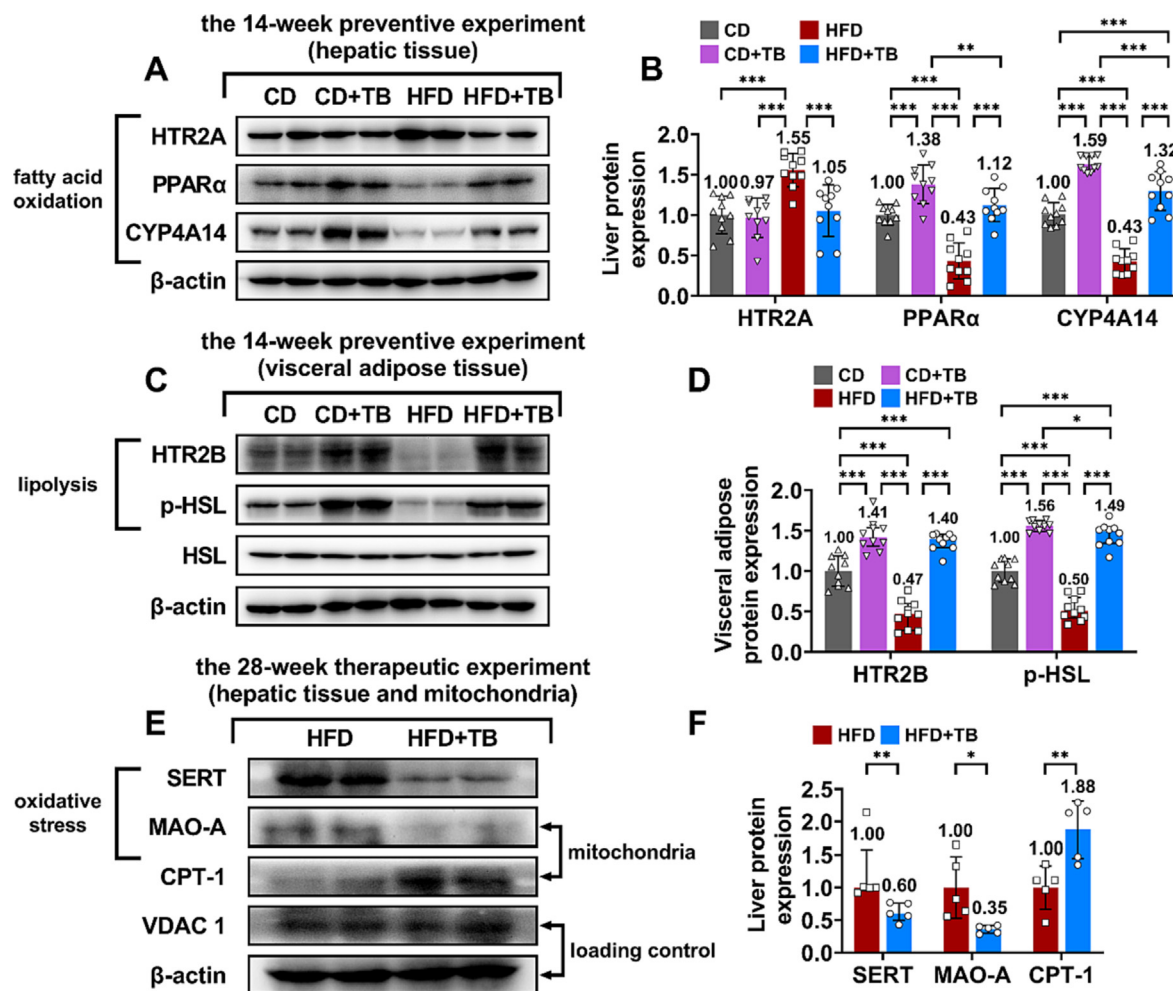
Fig. 4. TB alleviated NAFLD and obesity by regulating serotonin-related signaling pathways. (A) The western blot of HTR2A, PPARα and CYP4A14 in liver. **(B)** The expressions of target proteins in liver. **(C)** The western blot of HTR2B and HSL in visceral white adipose tissue. **(D)** The expressions of target proteins in visceral white adipose tissue. **(E)** The western blot of SERT, MAO-A and CPT-1 in hepatic tissue and hepatic mitochondria. **(F)** The expressions of target proteins in hepatic tissue and hepatic mitochondria. Data are shown as mean with SD or median with interquartile range, n = 5 or 10. Data were analyzed by either ANOVA, Kruskal-Wallis test, Student's *t*-test or Mann-Whitney *U* test. *P*-value < 0.05, **P*-value < 0.01, ***P*-value < 0.001. The symbols of triangle, inverted triangle, square and circle on the bars represent the samples of CD group, CD + TB group, HFD group, and HFD + TB groups, respectively. Abbreviation: ANOVA, analysis of variance; CD, control diet; CPT-1, carnitine palmitoyltransferase-1; CYP4A14, cytochrome P450 family of 4A14; HFD, high-fat diet; HTR2A, serotonin receptor 2A; HTR2B, serotonin receptor 2B; HSL, hormone-sensitive lipase; MAO-A, monoamine oxidase A; PPARα, peroxisome proliferator-activated receptor α; p-HSL, the phosphorylation of HSL; SD, standard deviation; SERT, serotonin transporter; TB, theabrownin; VDAC1, voltage-dependent anion-selective channel protein 1.

antibiotic cocktail was used to induce gut bacterial dysbiosis and change the gut microbial community (Fig. 6B-D). At the same time, the abundances of gut bacterial genera *Akkermansia*, *Bacteroides* and *Parabacteroides* were decreased after the intake of the antibiotic cocktail (Fig. 6E). Then, the antibiotics-induced gut bacterial dysbiosis increased the level of serotonin in liver, which was negatively correlated to the abundances of *Akkermansia* (r = -0.658), *Bacteroides* (r = -0.652) and *Parabacteroides* (r = -0.835) (Fig. 6F, G). Further, the gut bacterial dysbiosis increased the expressions of HTR2A and SERT while decreased the expressions of PPARα and CYP4A14 in liver (Fig. 6H, I).

To find out whether the beneficial regulation of TB on target proteins would regain following the restoration of gut microbiota or not, the original gut microbiota of C57BL/6J mice were firstly depleted, after that, the sterilized mice simultaneously received fecal microbiota transplant and TB intervention (Fig. 6A). The mice which did not receive antibiotic cocktail were chosen to be the donors for fecal microbiota (Fig. 6A). The evaluation of β-diversity based on the Bray-Curtis distance implied that there were significant differences in gut bacterial structure among groups

(Fig. 6C). Moreover, the evaluation of β-diversity based on weighted UniFrac distance showed that the dominant microbial taxonomy was conserved between the donor mice and the mice received fecal microbiota transplant (Fig. 6D). More importantly, following the restoration of *Akkermansia*, *Bacteroides* and *Parabacteroides*, the hepatic level of serotonin was decreased and the beneficial regulation of TB on HTR2A, PPARα, CYP4A14 and SERT in liver was regained (Fig. 6E, F, H, I).

In brief, the antibiotics-induced gut bacterial dysbiosis disrupted the regulation of TB on serotonin, HTR2A, PPARα, CYP4A14 and SERT in liver. Reversely, the beneficial regulation of TB on serotonin and related target proteins was regained with the restoration of gut microbiota. That is, TB relied on gut microbiota to regulate serotonin-related signaling pathways in liver.

Gut microbiota and TB co-contribute to alleviating NAFLD and obesity

To identify whether TB or gut microbiota was the key factor in alleviating NAFLD and obesity in this study, we conducted the fecal microbiota transplant without TB intervention. Referring to a pre-
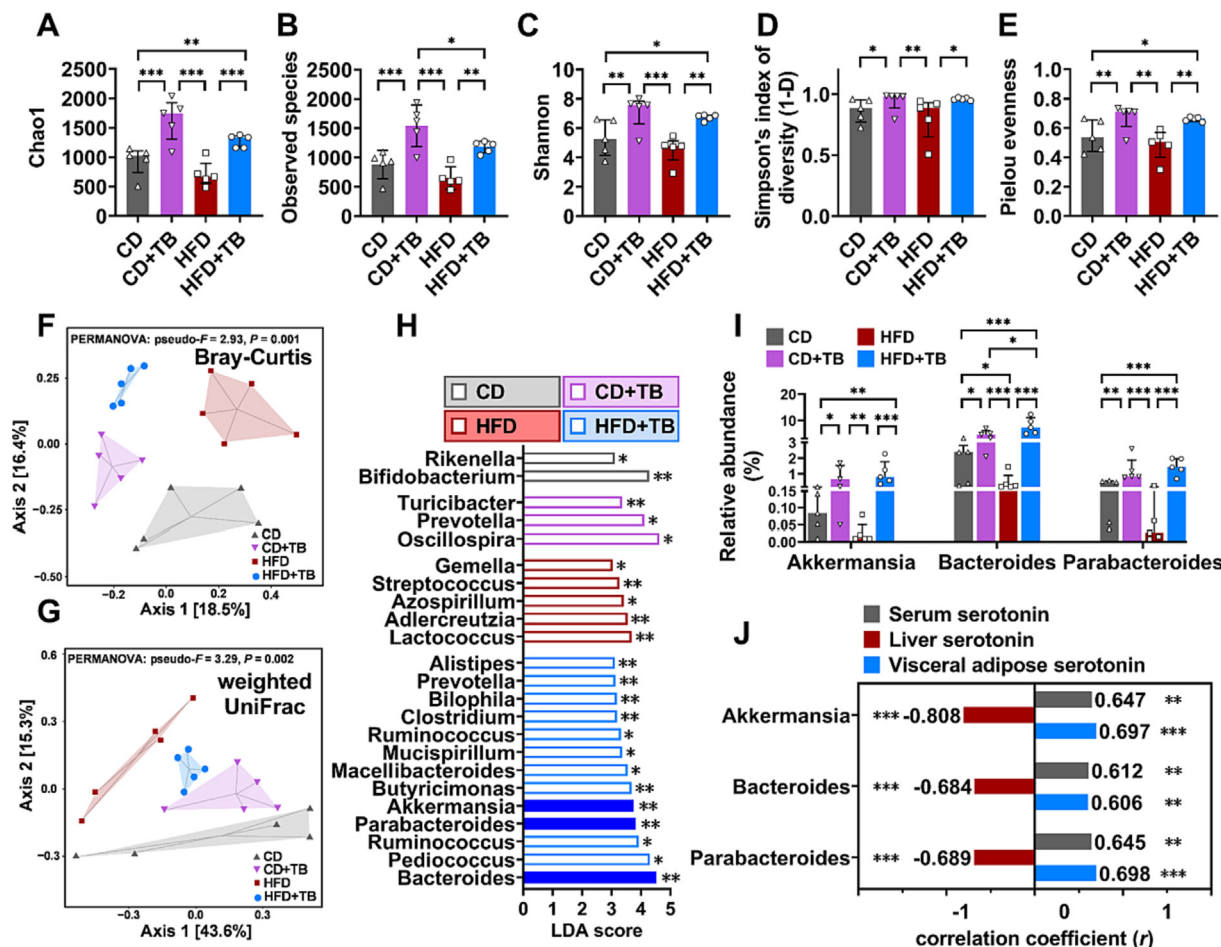
Fig. 5. The changes in gut microbiota from TB intervention and correlation analysis with serotonin. (A) Chao1 index for evaluating α-diversity. **(B)** Observed species richness for evaluating α-diversity. **(C)** Shannon index for evaluating α-diversity. **(D)** Simpson's index of diversity (also known as "1-D", a higher Simpson index means a higher α-diversity). **(E)** Pielou's evenness for evaluating α-diversity. **(F)** PCoA with Bray-Curtis distance for evaluating β-diversity. **(G)** PCoA with UniFrac distance for evaluating β-diversity. **(H)** The evaluation of LEfSe for gut microbiota. **(I)** The changes in abundances of the representative bacterial genera. **(J)** The Spearman correlation analysis between the representative bacterial genera and serotonin in different organs. Data are shown as mean with SD or median with interquartile range, n = 5. Data were analyzed by either ANOVA, Kruskal-Wallis test or PERMANOVA. *P-value < 0.05, **P-value < 0.01, ***P-value < 0.001. The symbols of triangle, inverted triangle, square and circle on the bars represent the samples of CD group, CD + TB group, HFD group, and HFD + TB group, respectively. Abbreviation: ANOVA, analysis of variance; CD, control diet; HFD, high-fat diet; LEfSe, linear discriminant analysis (LDA) effect size; PCoA, principal coordinate analysis; PERMANOVA, permutational multivariate analysis of variance; SD, standard deviation; TB, theabrownin.

vious study, the C57BL/6J mice were orally supplied with the antibiotic cocktail to deplete the original gut microbiota [30]. The simplified flow chart of the fecal microbiota experiment is exhibited in Fig. 7A. The feces collected from the HFD and HFD + TB groups in the 14-week preventive experiment were used to prepare fecal microbial supernatant for transplantation (Fig. 7A). Firstly, the content of fecal DNA extraction was extremely decreased by antibiotic cocktail supplement (Fig. S6). On the contrary, the fecal microbiota transplant significantly increased the content of fecal DNA extraction and the PCR amplification of gut bacterial 16S rRNA gene (Fig. S6). The transplantation of fecal microbiota derived from the HFD + TB group showed a better trend in preventing hepatic steatosis, body fat accumulation, and dyslipidemia than those from the HFD group (Fig. 7B-G). Besides, the combination of fecal microbiota and TB significantly alleviated hepatic steatosis and body fat accumulation compared with the transplantation of fecal microbiota alone (Fig. 7B). Also, the co-treatment decreased the level of TG in serum and liver (Fig. 7C, D). Moreover, the co-treatment decreased the levels of LDL-C and ALT in serum compared with fecal microbiota transplant alone (Fig. 7E, F). Furthermore, the co-treatment showed a better outcome in reducing the increase in body fat rate (Fig. 7G). Combining

the results from the antibiotic interference experiment and the fecal microbiota transplant experiment showed that gut microbiota and TB co-contributed to alleviating NAFLD and obesity in this study.

Discussion

The prevalence of NAFLD proportionately increased with the epidemics of obesity worldwide [48]. Under the global pandemic of COVID-19, the health burden of NAFLD and obesity becomes worse [49]. To overcome the challenge of NAFLD and obesity, we need to constantly explore better medicine. TB is a brown, water-soluble, macromolecular pigment converted from the oxidative polymerization of polyphenols (like catechins) and other substances (like polysaccharides and proteins) during the fermentation process of dark tea [50,51]. TB was consisted of phenolic acids, esters, proteins, and polysaccharides, and it could be stably extracted and isolated by a standardized and industrialized process using several steps of liquid–liquid extraction and precipitation processes with a variety of solvents [50]. Besides, TB is a safety substance with high bio-acceptability, and the median lethal dose (LD_{50}) of TB is greater than 10,000 mg/kg via gavage [26]. Sev-
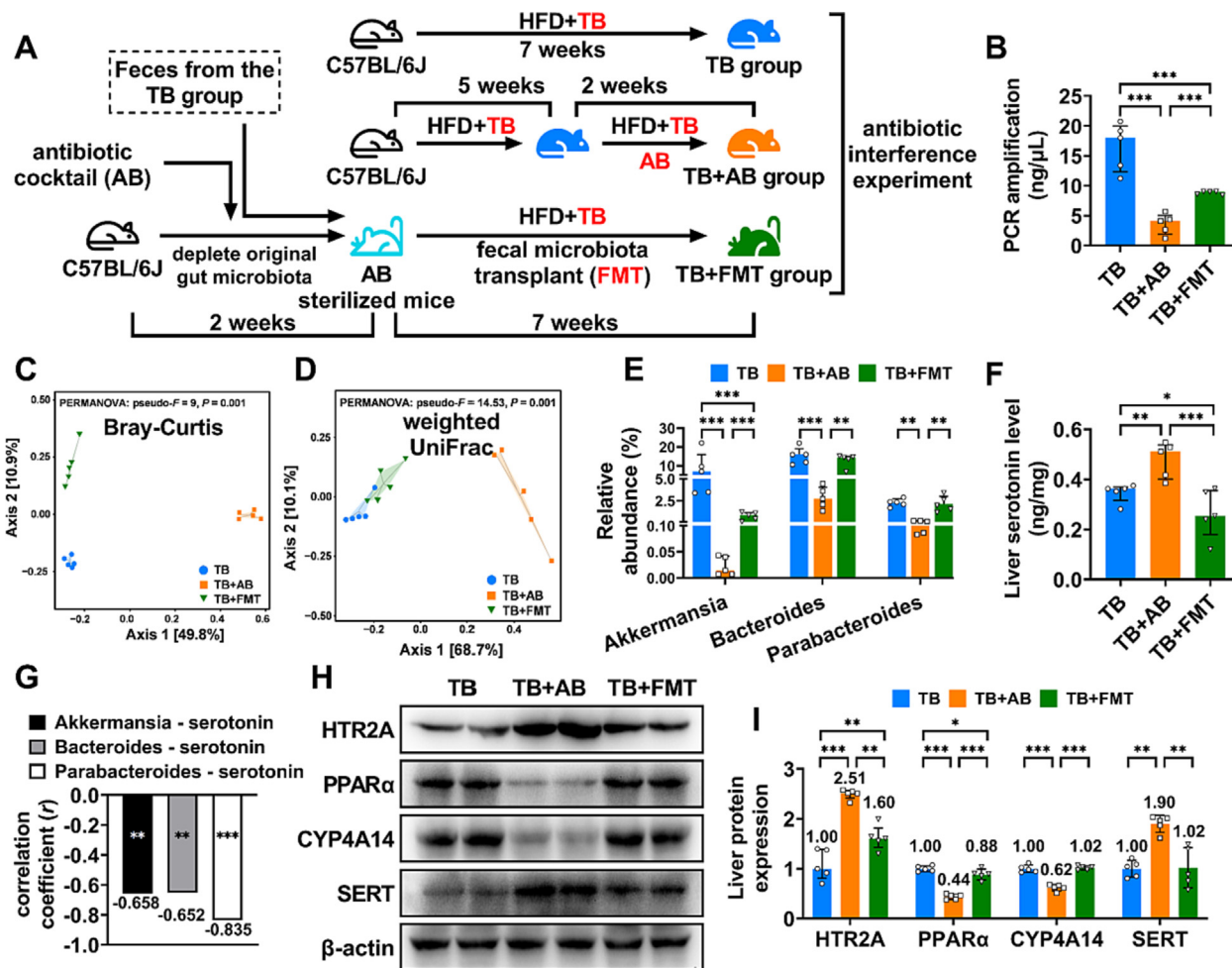
Fig. 6. The changes in gut microbiota and hepatic target proteins in the antibiotic interference experiment. (**A**) The simplified flow chart. The feces used for FMT were collected from the TB group. (**B**) The PCR amplification for 16S rRNA gene in feces. (**C**) PCoA with Bray-Curtis distance for evaluating β-diversity. (**D**) PCoA with UniFrac distance for evaluating β-diversity. (**E**) The changes in abundances of the representative bacterial genera. (**F**) The level of serotonin in liver. (**G**) The Spearman correlation analysis between the representative bacterial genera and serotonin in liver. (**H**) The western blot of HTR2A, PPARα, CYP4A14 and SERT in liver. (**I**) The relative quantification of target proteins in liver. Data are shown as mean with SD or median with interquartile range, n = 5. Data were analyzed by either ANOVA, Kruskal-Wallis test or PERMANOVA. *P-value < 0.05, **P-value < 0.01, ***P-value < 0.001. The symbols of circle, square, and inverted triangle on the bars represent the samples of TB group, TB + AB group, and TB + FMT group, respectively. Abbreviation: AB, antibiotic cocktail; ANOVA, analysis of variance; CYP4A14, cytochrome P450 family of 4A14; FMT, fecal microbiota transplant; HFD, high-fat diet; HTR2A, serotonin receptor 2A; PCoA, principal coordinate analysis; PCR, polymerase chain reaction; PERMANOVA, permutational multivariate analysis of variance; PPARα, peroxisome proliferator-activated receptor α; SD, standard deviation; SERT, serotonin transporter; TB, theabrownin.

eral studies reported that TB could inhibit osteoclast genesis, prevent bone loss, and induce apoptosis in osteosarcoma cells [52,53]. Also, TB showed anti-tumor activity on hepatocellular carcinoma [54]. However, the effect of TB on NAFLD is still a missing piece of the puzzle. In this study, the 14-week preventive experiment showed that TB intervention strongly prevented hepatic steatosis and reduced body weight gain (67.01 %), body fat rate (62.81 %) and hepatic TG level (51.35 %) compared with HFD-induced NAFLD model (Fig. 1). Comparing our findings with the results from other studies, TB could have more prominent and reliable effects on preventing fatty liver and obesity than other bioactive components of tea [16,55,56]. At the end of the 28-week therapeutic experiment, TB intervention reversed hepatic steatosis and decreased body weight (32.16 %), body fat rate (42.56 %) and hepatic TG level (42.86 %) (Fig. 2). Moreover, hepatic steatosis could lead to lipotoxicity and oxidative stress, which related to endoplasmic reticulum stress, mitochondrial dysfunction, and lysosomal dysfunction [10]. In this study, TB ameliorated oxidative stress in liver (Fig. 2). That is, TB could be a potential medicine for NAFLD and obesity treatment.

The previous study has reported that the gut-derived serotonin in portal blood was relatively higher than in peripheral blood, and serotonin could be an endocrine regulator [12]. In this study, we identified 243 differential metabolites among groups via untargeted metabolomic study, meanwhile, tryptophan metabolism pathway showed significant distinction between HFD group and HFD + TB group (Fig. 3). Referring to previous literature [57], the change in relative level of serotonin among groups highlighted that it could be the key molecule response to TB intervention. Untargeted metabolomics is a semiquantitative test, and ELISA is commonly used to further quantify the content of specific molecule [30,57,58]. In this study, the results of untargeted metabolomics and ELISA showed that TB decreased the level of serotonin in liver but increased the level of serotonin in blood circulation and visceral white adipose tissue (Fig. 3). The changes in serotonin distribution indicated that it could be a regulator for lipid metabolism (Figs. 1-3). Pathologically, the overexpression of HTR2A in liver has been considered as a risk factor for hepatic steatosis and fibrosis, whereas the liver-specific HTR2A knockout mice were resistant to hepatic steatosis with increasing the expression of downstream proteins like PPARα [12,13,59]. Further, PPARα is one of the pivotal
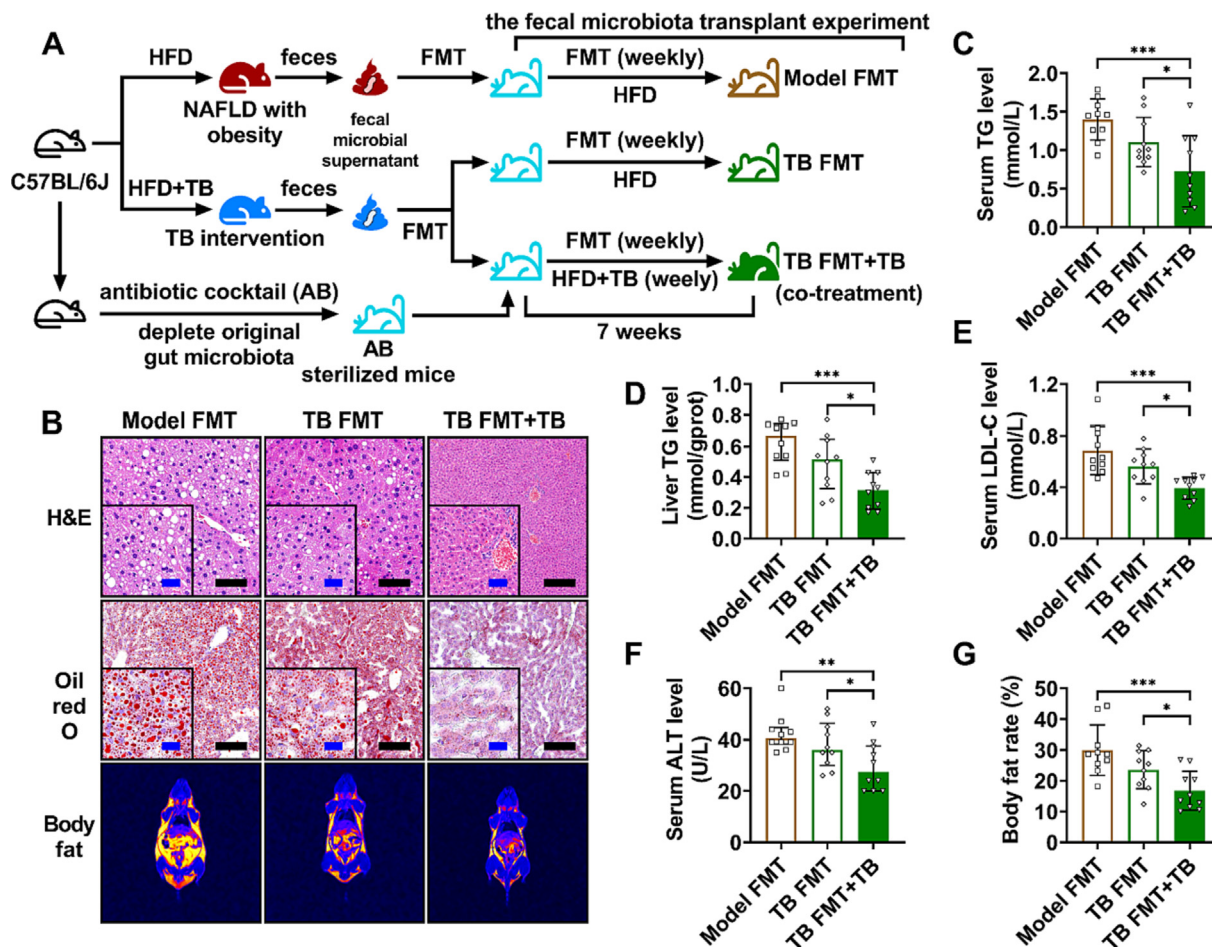
Fig. 7. The effects of fecal microbiota transplant on NAFLD and obesity. (A) The simplified flow chart. The feces used to FMT were collected from the HFD and HFD + TB groups in the 14-week preventive experiment. **(B)** Hepatic H&E and Oil red O staining (black scale bar = 200 μm and blue scale bar = 50 μm), and body fat distribution scanned by NMR (the adipose tissue is highlighted). **(C)** The level of TG in serum. **(D)** The level of TG in liver. **(E)** The level of LDL-C in serum. **(F)** The level of ALT in serum. **(G)** Body fat rate. Data are shown as mean with SD or median with interquartile range, n = 10. Data were analyzed by either ANOVA or Kruskal-Wallis test. *P-value < 0.05, **P-value < 0.01, ***P-value < 0.001. The symbols of square, rhombus, and inverted triangle on the bars represent the samples of Model FMT group, TB FMT group, and TB FMT + TB group, respectively. Abbreviation: AB, antibiotic cocktail; ALT, alanine aminotransferase; ANOVA, analysis of variance; FMT, fecal microbiota transplant; H&E, hematoxylin and eosin; HFD, high-fat diet; LDL-C, low-density lipoprotein cholesterol; NMR, nuclear magnetic resonance; SD, standard deviation; TB, theabrownin; TG, triglyceride.

lipolytic genes, which could promote fatty acid oxidation by increasing the expression of downstream molecules like CYP4A14 and CPT-1 [36,60,61]. Mechanistically, we proved that TB promoted fatty acid oxidation by decreasing the expression of HTR2A while increasing the expressions of PPARα, CYP4A14 and CPT-1 in liver (Fig. 4A, B). Besides, previous studies have reported that HTR2B was the dominant serotonin receptor in visceral white adipose tissue of mice, and the upregulated expression of HTR2B in adipocytes could promote lipolysis by activating HSL [14,62]. In this study, TB promoted lipolysis by activating the HTR2B-HSL signaling pathway (Fig. 4C, D). Additionally, previous studies indicated that the upregulation of the SERT-MAO-A signaling pathway could lead to the excessive degradation of serotonin in liver and further induce the overproduction of ROS in hepatic mitochondria [33,63]. In this study, TB mitigated oxidative stress by inhibiting the SERT-MAO-A signaling pathway in liver (Fig. 4E, F). In short, TB alleviates NAFLD and obesity by regulating the HTR2A-PPARα-CYP4A14/CPT-1 and SERT-MAO-A signaling pathways in liver, and the HTR2B-HSL signaling pathway in visceral white adipose tissue.

The relationship among gut microbiota, NAFLD and obesity has been widely concerned [64]. For example, gut bacterial dysbiosis is common in patient with NAFLD and obesity, and the relative abundance of *Streptococcus* was increased while that of *Akkermansia* was decreased in fecal sample [65,66]. Moreover, previous litera-

ture reported that the relative abundance of *Akkermansia muciniphila* in NAFLD mice was significantly decreased, which induced the dysfunction of intestinal barrier, elevated the level of lipopolysaccharide in circulation, and finally provoked systematic inflammation [67]. Furthermore, previous studies had reported that gut microbiota could regulate the synthesis of serotonin in the enterochromaffin cells [68]. However, whether gut microbiota could affect the content and function of serotonin in liver is unknown. In this study, TB alleviated gut bacterial dysbiosis and increased the richness and evenness of gut microbiota, reflecting in increasing the indexes of α-diversity (like Chao1, observed species richness, Shannon index, Simpson's index of diversity, and Pielou's evenness) (Fig. 5). Also, the evaluation of β-diversity implied that TB changed the structure of gut microbial community (Fig. 5). Moreover, TB increased the abundances of gut bacterial genera *Akkermansia*, *Bacteroides* and *Parabacteroides*, which were negatively correlated to the level of serotonin in liver while positively correlated to the level of serotonin in blood circulation and visceral adipose white tissue (Fig. 5). In short, our findings suggested that TB intervention could effectively alleviate gut bacterial dysbiosis in mice with NAFLD and obesity. Other literature has recommended that the intake of probiotics (like *Akkermansia muciniphila*), prebiotics (like inulin oligofructose) and symbiotics (like the combination of *Bacillus licheniformis* and xylooligosaccharides) could be beneficial for the prevention and treat-
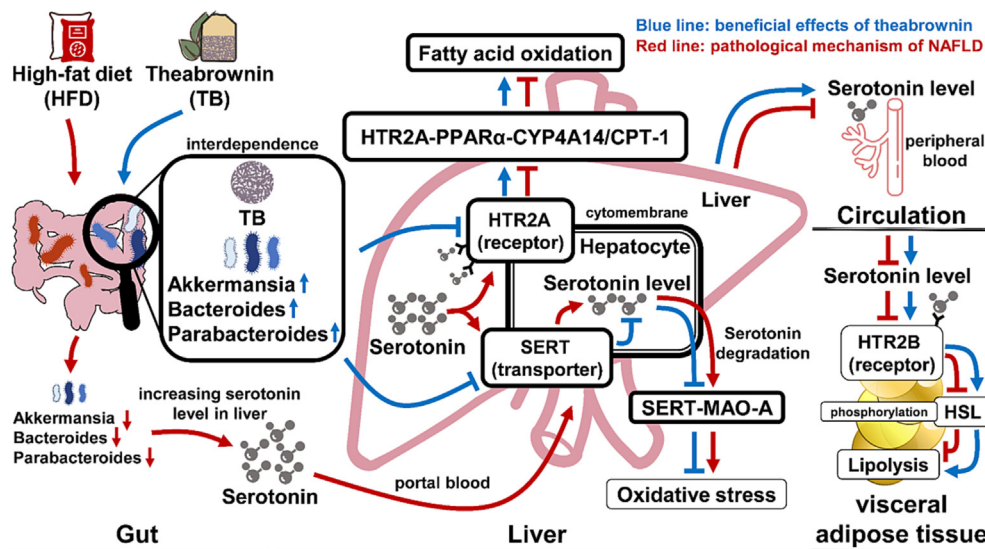
Fig. 8. The proposed mechanism of TB to alleviate NAFLD and obesity. The HFD was used to induce NAFLD and obesity. TB could alleviate NAFLD and obesity based on the following mechanisms: (1) TB decreased the level of serotonin in liver while increased the level of serotonin in blood circulation and visceral white adipose tissue. (2) TB promoted fatty acid oxidation in liver by decreasing the expression of HTR2A and increasing the expressions of downstream molecules, including PPARα, CYP4A14 and CPT-1. (3) TB reduced the excessive degradation of serotonin to mitigate oxidative stress in liver by decreasing the expression of SERT and MAO-A. (4) Serotonin could be circulated to visceral white adipose tissue and promote lipolysis by activating HTR2B and HSL. (5) TB increased the abundances of gut bacterial genera *Akkermansia*, *Bacteroides* and *Parabacteroides*. (6) The regulation of TB on HTR2A, PPARα, CYP4A14 and SERT needed the participation of gut microbiota (such as *Akkermansia*, *Bacteroides* and *Parabacteroides*). Moreover, fecal microbiota transplant indicated that TB and gut microbiota co-contributed to alleviating NAFLD and obesity. Together, TB alleviated NAFLD and obesity by regulating serotonin-related signaling pathways in a gut microbiota-dependent manner. Abbreviation: CPT-1, carnitine palmitoyltransferase-1; CYP4A14, cytochrome P450 family of 4A14; HFD, high-fat diet; HSL, hormone-sensitive lipase; HTR2A, serotonin receptor 2A; HTR2B, serotonin receptor 2B; NAFLD, non-alcoholic fatty liver disease; MAO-A, monoamine oxidase A; SERT, serotonin transporter; TB, theabrownin; PPARα, peroxisome proliferator-activated receptor α.

ment of NAFLD and obesity [69,70]. So, the regulation of gut microbiota could be one of the important mechanisms for TB to alleviate NAFLD and obesity, and the co-treatment of TB and probiotics/prebiotics (like medicinal plants [71,72]) is worthy to be further explored.

In the literature, antibiotics sterilized mice and germ-free mice were widely used to study the function of gut microbiota [7,32,58,73]. In this study, we used antibiotic cocktail to verify the role of gut microbiota for TB in alleviating NAFLD. The results showed that TB relied on gut microbiota to regulate serotonin level and related target proteins in liver, meanwhile, gut microbiota and TB co-contributed to alleviating NAFLD and obesity (Figs. 6, 7). These findings confirmed the positive role of *Akkermansia*, *Bacteroides* and *Parabacteroides* in alleviating NAFLD and obesity, and proposed novel insight into the relationship among TB, serotonin, gut microbiota, and NAFLD [32,69,74]. At last, because the alleviation of hepatic steatosis and body fat accumulation is a dominant approach for NAFLD and obesity, further clinical trials are worthy to explore the effect of TB on patients [4,37]. The effects of TB on visceral fat inflammation and systemic metabolic dysregulation might be also explored in the future. Besides, TB is one of the main bioactive components generated from the fermentation of dark tea, whether the optimization of the fermented process could improve the bioactive effects of TB on NAFLD and obesity is worth further investigation [75]. In addition, untargeted metabolomic analysis could be performed on feces, and the correlation between fecal metabolites and the changes in the composition of gut microbiota should be analyzed.

Conclusions

Our study reveals that TB has significantly preventive and therapeutic effects on NAFLD and obesity by regulating serotonin-related signaling pathways. Moreover, the beneficial regulation of TB on serotonin level and related target proteins in liver relies on

the participation of gut microbiota, meanwhile, TB and gut microbiota co-contributed to alleviating NAFLD and obesity. The proposed mechanisms are exhibited in Fig. 8. Our findings bring novel insight into the relationship among TB, serotonin, gut microbiota, NAFLD, and obesity. At the same time, this study provides a reference for subsequent clinical trials, and hopefully, TB is a promising medicine for reducing the global burden of NAFLD and obesity.

Ethics statement

All experiments in this study were conducted according to the national legislation and the guidelines of the laboratory animal center at Sun Yat-Sen University (Guangzhou, China). All experimental procedures were approved by the Ethics Committee in the School of Public Health, Sun Yat-Sen University (No. 2019-002).

Compliance with ethics requirements

Animal studies were reported in compliance with the ARRIVE guidelines. All experimental procedures were approved by the Ethics Committee in the School of Public Health, Sun Yat-Sen University (No. 2019-002). All experiments in this study were conducted according to the national legislation, the guidelines of the laboratory animal center at Sun Yat-Sen University , and the Guide for the Care and Use of Laboratory Animals from the National Institutes of Health (the eighth edition).

CRediT authorship contribution statement

Hang-Yu Li: Conceptualization, Methodology, Formal analysis, Investigation, Data curation, Software, Visualization, Writing – original draft. **Si-Yu Huang:** Methodology, Software, Investigation. **Dan-Dan Zhou:** Software, Investigation. **Ruo-Gu Xiong:** Formal analysis, Investigation. **Min Luo:** Formal analysis, Data curation.

Adila Saimaiti: Data acquisition, Data analysis. **Mu-Ke Han:** Visualization, Data curation. **Ren-You Gan:** Conceptualization, Supervision, Visualization, Writing – review & editing. **Hui-Lian Zhu:** Methodology, Writing – review & editing. **Hua-Bin Li:** Conceptualization, Project administration, Supervision, Writing – review & editing.

Declaration of Competing Interest

The authors declare that they have no known competing financial interests or personal relationships that could have appeared to influence the work reported in this paper.

Acknowledgments

Appendix A. Supplementary material

Supplementary data to this article can be found online at https://doi.org/10.1016/j.jare.2023.01.008.

References

[1] Vily-Petit J, Soty-Roca M, Silva M, Raffin M, Gautier-Stein A, Rajas F, et al. Intestinal gluconeogenesis prevents obesity-linked liver steatosis and non-alcoholic fatty liver disease. Gut 2020;69(12):2193–202. doi: https://doi.org/10.1136/gutjnl-2019-319745.

[2] Powell EE, Wong VW, Rinella M. Non-alcoholic fatty liver disease. Lancet 2021;397(10290):2212–24. doi: https://doi.org/10.1016/S0140-6736(20)32511-3.

[3] Younossi ZM, Koenig AB, Abdelatif D, Fazel Y, Henry L, Wymer M. Global epidemiology of nonalcoholic fatty liver disease-Meta-analytic assessment of prevalence, incidence, and outcomes. Hepatology 2016;64(1):73–84. doi: https://doi.org/10.1002/hep.28431.

[4] Rotman Y, Sanyal AJ. Current and upcoming pharmacotherapy for non-alcoholic fatty liver disease. Gut 2017;66(1):180–90. doi: https://doi.org/10.1136/gutjnl-2016-312431.

[5] Esler WP, Bence KK. Metabolic targets in nonalcoholic fatty liver disease. Cell Mol Gastroenterol Hepatol 2019;8(2):247–67. doi: https://doi.org/10.1016/j.jcmgh.2019.04.007.

[6] Cohen JC, Horton JD, Hobbs HH. Human fatty liver disease: old questions and new insights. Science 2011;332(6037):1519–23. doi: https://doi.org/10.1126/science.1204265.

[7] Le Roy T, Llopis M, Lepage P, Bruneau A, Rabot S, Bevilacqua C, et al. Intestinal microbiota determines development of non-alcoholic fatty liver disease in mice. Gut 2013;62(12):1787–94. doi: https://doi.org/10.1136/gutjnl-2012-303816.

[8] Meng X, Li S, Li Y, Gan RY, Li HB. Gut microbiota's relationship with liver disease and role in hepatoprotection by dietary natural products and probiotics. Nutrients 2018;10(10):1457. doi: https://doi.org/10.3390/nu10101457.

[9] Zhang YJ, Li S, Gan RY, Zhou T, Xu DP, Li HB. Impacts of gut bacteria on human health and diseases. Int J Mol Sci 2015;16(4):7493–519. doi: https://doi.org/10.3390/ijms16047493.

[10] Geng Y, Faber KN, de Meijer VE, Blokzijl H, Moshage H. How does hepatic lipid accumulation lead to lipotoxicity in non-alcoholic fatty liver disease? Hepatol Int 2021;15(1):21–35. doi: https://doi.org/10.1007/s12072-020-10121-2.

[11] Agus A, Planchais J, Sokol H. Gut microbiota regulation of tryptophan metabolism in health and disease. Cell Host Microbe 2018;23(6):716–24. doi: https://doi.org/10.1016/j.chom.2018.05.003.

[12] Yabut JM, Crane JD, Green AE, Keating DJ, Khan WI, Steinberg GR. Emerging roles for serotonin in regulating metabolism: New implications for an ancient molecule. Endocr Rev 2019;40(4):1092–107. doi: https://doi.org/10.1210/er.2018-00283.

[13] Choi W, Namkung J, Hwang I, Kim H, Lim A, Park HJ, et al. Serotonin signals through a gut-liver axis to regulate hepatic steatosis. Nat Commun 2018;9:4824. doi: https://doi.org/10.1038/s41467-018-07287-7.

[14] Sumara G, Sumara O, Kim JK, Karsenty G. Gut-derived serotonin is a multifunctional determinant to fasting adaptation. Cell Metab 2012;16 (5):588–600. doi: https://doi.org/10.1016/j.cmet.2012.09.014.

[15] Yano JM, Yu K, Donaldson GP, Shastri GG, Ann P, Ma L, et al. Indigenous bacteria from the gut microbiota regulate host serotonin biosynthesis. Cell 2015;161(2):264–76. doi: https://doi.org/10.1016/j.cell.2015.02.047.

[16] Li HY, Gan RY, Shang A, Mao QQ, Sun QC, Wu DT, et al. Plant-based foods and their bioactive compounds on fatty liver disease: Effects, mechanisms, and clinical application. Oxidative Med Cell Longev 2021;2021:6621644. doi: https://doi.org/10.1155/2021/6621644.

[17] Zhao CN, Tang GY, Cao SY, Xu XY, Gan RY, Liu Q, et al. Phenolic profiles and antioxidant activities of 30 tea infusions from green, black, oolong, white, yellow and dark teas. Antioxidants 2019;8(7):215. doi: https://doi.org/10.3390/antiox8070215.

[18] Zeng L, Yan J, Luo L, Zhang D. Effects of Pu-erh tea aqueous extract (PTAE) on blood lipid metabolism enzymes. Food Funct 2015;6(6):2008–16. doi: https://doi.org/10.1039/c5fo00362h.

[19] Wang SA, Qiu Y, Gan RY, Zhu F. Chemical constituents and biological properties of Pu-erh tea. Food Res Int 2022;154:. doi: https://doi.org/10.1016/j.foodres.2021.110899110899.

[20] Kuo KL, Weng MS, Chiang CT, Tsai YJ, Lin-Shiau SY, Lin JK. Comparative studies on the hypolipidemic and growth suppressive effects of oolong, black, pu-erh, and green tea leaves in rats. J Agric Food Chem 2005;53(2):480–9. doi: https://doi.org/10.1021/jf049375k.

[21] Cao SY, Li BY, Gan RY, Mao QQ, Wang YF, Shang A, et al. The in vivo antioxidant and hepatoprotective actions of selected Chinese teas. Foods 2020;9(3):262. doi: https://doi.org/10.3390/foods9030262.

[22] Mao QQ, Li BY, Meng JM, Gan RY, Xu XY, Gu YY, et al. Effects of several tea extracts on nonalcoholic fatty liver disease in mice fed with a high-fat diet. Food Sci Nutr 2021;9(6):2954–67. doi: https://doi.org/10.1002/fsn3.2255.

[23] Lin FJ, Wei XL, Liu HY, Li H, Xia Y, Wu DT, et al. State-of-the-art review of dark tea: From chemistry to health benefits. Trends Food Sci Technol 2021;109:126–38. doi: https://doi.org/10.1016/j.tifs.2021.01.030.

[24] Brandsma E, Kloosterhuis NJ, Koster M, Dekker DC, Gijbels MJJ, van der Velden S, et al. A proinflammatory gut microbiota increases systemic inflammation and accelerates atherosclerosis. Circ Res 2019;124(1):94–100. doi: https://doi.org/10.1161/CIRCRESAHA.118.313234.

[25] Yu L, Wang L, Yi H, Wu X. Beneficial effects of LRP6-CRISPR on prevention of alcohol-related liver injury surpassed fecal microbiota transplant in a rat model. Gut Microbes 2020;11(4):1015–29. doi: https://doi.org/10.1080/19490976.2020.1736457.

[26] Yue S, Zhao D, Peng C, Tan C, Wang Q, Gong J. Effects of theabrownin on serum metabolites and gut microbiome in rats with a high-sugar diet. Food Funct 2019;10(11):7063–80. doi: https://doi.org/10.1039/c9fo01334b.

[27] Reagan-Shaw S, Nihal M, Ahmad N. Dose translation from animal to human studies revisited. FASEB J 2008;22(3):659–61. doi: https://doi.org/10.1096/fj.07-9574LSF.

[28] Benakis C, Brea D, Caballero S, Faraco G, Moore J, Murphy M, et al. Commensal microbiota affects ischemic stroke outcome by regulating intestinal gammadelta T cells. Nat Med 2016;22(5):516–23. doi: https://doi.org/10.1038/nm.4068.

[29] Liang WO, Zhao LC, Zhang JF, Fang X, Zhong QP, Liao ZL, et al. Colonization potential to reconstitute a microbe community in pseudo germ-free mice after fecal microbe transplant from equol producer. Front Microbiol 2020;11:1221. doi: https://doi.org/10.3389/fmicb.2020.01221.

[30] Gong S, Lan T, Zeng L, Luo H, Yang X, Li N, et al. Gut microbiota mediates diurnal variation of acetaminophen induced acute liver injury in mice. J Hepatol 2018;69(1):51–9. doi: https://doi.org/10.1016/j.jhep.2018.02.024.

[31] Matsui M, Fukunishi S, Nakano T, Ueno T, Higuchi K, Asai A. Ileal bile acid transporter inhibitor improves hepatic steatosis by ameliorating gut microbiota dysbiosis in NAFLD model mice. MBio 2021;12(4): e01155–10221. doi: https://doi.org/10.1128/mBio.01155-21.

[32] Zhang X, Coker OO, Chu ES, Fu K, Lau HCH, Wang YX, et al. Dietary cholesterol drives fatty liver-associated liver cancer by modulating gut microbiota and metabolites. Gut 2021;70(4):761–74. doi: https://doi.org/10.1136/gutjnl-2019-319664.

[33] Fu J, Li C, Zhang G, Tong X, Zhang H, Ding J, et al. Crucial roles of 5-HT and 5-HT2 receptor in diabetes-related lipid accumulation and pro-inflammatory cytokine generation in hepatocytes. Cell Physiol Biochem 2018;48 (6):2409–28. doi: https://doi.org/10.1159/000492656.

[34] Chiang MK, Hsiao PY, Liu YY, Tang HL, Chiou CS, Lu MC, et al. Two ST11 Klebsiella pneumoniae strains exacerbate colorectal tumorigenesis in a colitis-associated mouse model. Gut Microbes 2021;13(1):1980348. doi: https://doi.org/10.1080/19490976.2021.1980348.

[35] Lee SM, Pusec CM, Norris GH, De Jesus A, Diaz-Ruiz A, Muratalla J, et al. Hepatocyte-specific loss of PPARgamma protects mice from NASH and increases the therapeutic effects of rosiglitazone in the liver. Cell Mol Gastroenterol Hepatol 2021;11(5):1291–311. doi: https://doi.org/10.1016/j.jcmgh.2021.01.003.

[36] Yang Z, Li P, Shang Q, Wang Y, He J, Ge S, et al. CRISPR-mediated BMP9 ablation promotes liver steatosis via the down-regulation of PPAR alpha expression. Sci Adv 2020;6(48):eabc5022. doi: https://doi.org/10.1126/sciadv.abc5022.

[37] Li HY, Huang SY, Xiong RG, Wu SX, Zhou DD, Saimaiti A, et al. Anti-obesity effect of theabrownin from dark tea in C57BL/6J mice fed a high-fat diet by metabolic profiles through gut microbiota using untargeted metabolomics. Foods 2022;11(19):3000. doi: https://doi.org/10.3390/foods11193000.

[38] Li B, Mao Q, Zhou D, Luo M, Gan R, Li H, et al. Effects of tea against alcoholic fatty liver disease by modulating gut microbiota in chronic alcohol-exposed mice. Foods 2021;10(6):1232. doi: https://doi.org/10.3390/foods10061232.

[39] Zhuang P, Li HY, Jia W, Shou QY, Zhu YE, Mao L, et al. Eicosapentaenoic and docosahexaenoic acids attenuate hyperglycemia through the microbiome-gut-

organs axis in db/db mice. Microbiome 2021;9(1):185. doi: https://doi.org/10.1186/s40168-021-01126-6.

[40] Frantsiyants EM, Bandovkina VA, Kaplieva IV, Surikova EI, Neskubina IV, Cheryarina ND, et al. Chronic neurogenic pain is responsible for changes in concentrations of biogenic amines in the brain in urokinase knockout mice with melanoma B16/F10. Cardiometry 2020;17:49–57. doi: https://doi.org/10.12710/cardiometry.2020.17.49-57.

[41] Mootha VK, Bunkenborg J, Olsen JV, Hjerrild M, Wisniewski JR, Stahl E, et al. Integrated analysis of protein composition, tissue diversity, and gene regulation in mouse mitochondria. Cell 2003;115(5):629–40. doi: https://doi.org/10.1016/s0092-8674(03)00926-7.

[42] Wang WC, Zhai SS, Xia YY, Wang H, Ruan D, Zhou T, et al. Ochratoxin A induces liver inflammation: involvement of intestinal microbiota. Microbiome 2019;7(1):151. doi: https://doi.org/10.1186/s40168-019-0761-z.

[43] Carpino G, Del Ben M, Pastori D, Carnevale R, Baratta F, Overi D, et al. Increased liver localization of lipopolysaccharides in human and experimental NAFLD. Hepatology 2020;72(2):470–85. doi: https://doi.org/10.1002/hep.31056.

[44] Han Q, Wang J, Li W, Chen ZJ, Du Y. Androgen-induced gut dysbiosis disrupts glucolipid metabolism and endocrinal functions in polycystic ovary syndrome. Microbiome 2021;9(1):101. doi: https://doi.org/10.1186/s40168-021-01046-5.

[45] Lei Y, Tang L, Liu S, Hu S, Wu L, Liu Y, et al. Parabacteroides produces acetate to alleviate heparanase-exacerbated acute pancreatitis through reducing neutrophil infiltration. Microbiome 2021;9(1):115. doi: https://doi.org/10.1186/s40168-021-01065-2.

[46] Tilocca B, Burbach K, Heyer CME, Hoelzle LE, Mosenthin R, Stefanski V, et al. Dietary changes in nutritional studies shape the structural and functional composition of the pigs' fecal microbiome-from days to weeks. Microbiome 2017;5(1):144. doi: https://doi.org/10.1186/s40168-017-0362-7.

[47] Soto M, Herzog C, Pacheco JA, Fujisaka S, Bullock K, Clish CB, et al. Gut microbiota modulate neurobehavior through changes in brain insulin sensitivity and metabolism. Mol Psychiatr 2018;23(12):2287–301. doi: https://doi.org/10.1038/s41380-018-0086-5.

[48] Younossi ZM. Non-alcoholic fatty liver disease - A global public health perspective. J Hepatol 2019;70(3):531–44. doi: https://doi.org/10.1016/j.jhep.2018.10.033.

[49] Stefan N, Birkenfeld AL, Schulze MB. Global pandemics interconnected - obesity, impaired metabolic health and COVID-19. Nat Rev Endocrinol 2021;17(3):135–49. doi: https://doi.org/10.1038/s41574-020-00462-1.

[50] Long P, Wen M, Granato D, Zhou J, Wu Y, Hou Y, et al. Untargeted and targeted metabolomics reveal the chemical characteristic of Pu-erh tea (Camellia assamica) during pile-fermentation. Food Chem 2020;311:. doi: https://doi.org/10.1016/j.foodchem.2019.125895125895.

[51] Zhu MZ, Li N, Zhou F, Ouyang J, Lu DM, Xu W, et al. Microbial bioconversion of the chemical components in dark tea. Food Chem 2020;312:. doi: https://doi.org/10.1016/j.foodchem.2019.126043126043.

[52] Liu T, Xiang Z, Chen F, Yin D, Huang Y, Xu J, et al. Theabrownin suppresses in vitro osteoclastogenesis and prevents bone loss in ovariectomized rats. Biomed Pharmacother 2018;106:1339–47. doi: https://doi.org/10.1016/j.biopha.2018.07.103.

[53] Jin W, Zhou L, Yan B, Yan L, Liu F, Tong P, et al. Theabrownin triggers DNA damage to suppress human osteosarcoma U2OS cells by activating p53 signalling pathway. J Cell Mol Med 2018;22(9):4423–36. doi: https://doi.org/10.1111/jcmm.13742.

[54] Xu J, Yan B, Zhang L, Zhou L, Zhang J, Yu W, et al. Theabrownin induces apoptosis and tumor inhibition of hepatocellular carcinoma Huh7 cells through ASK1-JNK-c-Jun pathway. OncoTargets Ther 2020;13:8977–87. doi: https://doi.org/10.2147/OTT.S254693.

[55] Masterjohn C, Bruno RS. Therapeutic potential of green tea in nonalcoholic fatty liver disease. Nutr Rev 2012;70(1):41–56. doi: https://doi.org/10.1111/j.1753-4887.2011.00440.x.

[56] Liang J, Gu L, Liu X, Yan X, Bi X, Fan X, et al. L-theanine prevents progression of nonalcoholic hepatic steatosis by regulating hepatocyte lipid metabolic pathways via the CaMKK beta-AMPK signaling pathway. Nutr Metab 2022;19(1):29. doi: https://doi.org/10.1186/s12986-022-00664-6.

[57] Nemet I, Saha PP, Gupta N, Zhu W, Romano KA, Skye SM, et al. A cardiovascular disease-linked gut microbial metabolite acts via adrenergic receptors. Cell 2020;180(5):862–77. doi: https://doi.org/10.1016/j.cell.2020.02.016.

[58] Fung TC, Vuong HE, Luna CDG, Pronovost GN, Aleksandrova AA, Riley NG, et al. Intestinal serotonin and fluoxetine exposure modulate bacterial colonization in the gut. Nat Microbiol 2019;4(12):2064–73. doi: https://doi.org/10.1038/s41564-019-0540-4.

[59] Wang L, Fan X, Han J, Cai M, Wang X, Wang Y, et al. Gut-derived serotonin contributes to the progression of non-alcoholic steatohepatitis via the liver HTR2A/PPARgamma2 pathway. Front Pharmacol 2020;11:553. doi: https://doi.org/10.3389/fphar.2020.00553.

[60] Xu B, Jiang M, Chu Y, Wang W, Chen D, Li X, et al. Gasdermin D plays a key role as a pyroptosis executor of non-alcoholic steatohepatitis in humans and mice. J Hepatol 2018;68(4):773–82. doi: https://doi.org/10.1016/j.jhep.2017.11.040.

[61] Chen X, Zhang F, Gong Q, Cui A, Zhuo S, Hu Z, et al. Hepatic ATF6 increases fatty acid oxidation to attenuate hepatic steatosis in mice through peroxisome proliferator-activated receptor alpha. Diabetes 2016;65(7):1904–15. doi: https://doi.org/10.2337/db15-1637.

[62] Meltzer HY, Roth BL. Lorcaserin and pimavanserin: emerging selectivity of serotonin receptor subtype-targeted drugs. J Clin Invest 2013;123(12):4986–91. doi: https://doi.org/10.1172/JCI70678.

[63] Nocito A, Dahm F, Jochum W, Jang JH, Georgiev P, Bader M, et al. Serotonin mediates oxidative stress and mitochondrial toxicity in a murine model of nonalcoholic steatohepatitis. Gastroenterology 2007;133(2):608–18. doi: https://doi.org/10.1053/j.gastro.2007.05.019.

[64] Fan Y, Pedersen O. Gut microbiota in human metabolic health and disease. Nat Rev Microbiol 2021;19(1):55–71. doi: https://doi.org/10.1038/s41579-020-0433-9.

[65] Aron-Wisnewsky J, Vigliotti C, Witjes J, Le P, Holleboom AG, Verheij J, et al. Gut microbiota and human NAFLD: disentangling microbial signatures from metabolic disorders. Nat Rev Gastroenterol Hepatol 2020;17(5):279–97. doi: https://doi.org/10.1038/s41575-020-0269-9.

[66] Ponziani FR, Bhoori S, Castelli C, Putignani L, Rivoltini L, Del Chierico F, et al. Hepatocellular carcinoma is associated with gut microbiota profile and inflammation in nonalcoholic fatty liver disease. Hepatology 2019;69(1):107–20. doi: https://doi.org/10.1002/hep.30036.

[67] Shi Z, Lei H, Chen G, Yuan P, Cao Z, Ser HL, et al. Impaired intestinal Akkermansia muciniphila and aryl hydrocarbon receptor ligands contribute to nonalcoholic fatty liver disease in mice. mSystems 2021;6(1):e00985–e1020. doi: https://doi.org/10.1128/mSystems.00985-20.

[68] Stasi C, Sadalla S, Milani S. The relationship between the serotonin metabolism, gut-microbiota and the gut-brain axis. Curr Drug Metab 2019;20(8):646–55. doi: https://doi.org/10.2174/1389200220666190725115503.

[69] Rao Y, Kuang Z, Li C, Guo S, Xu Y, Zhao D, et al. Gut Akkermansia muciniphila ameliorates metabolic dysfunction-associated fatty liver disease by regulating the metabolism of L-aspartate via gut-liver axis. Gut Microbes 2021;13(1):1927633. doi: https://doi.org/10.1080/19490976.2021.1927633.

[70] Li HY, Zhou DD, Gan RY, Huang SY, Zhao CN, Shang A, et al. Effects and mechanisms of probiotics, prebiotics, synbiotics, and postbiotics on metabolic diseases targeting gut microbiota: A narrative review. Nutrients 2021;13(9):3211. doi: https://doi.org/10.3390/nu13093211.

[71] El Seedy GM, El-Shafey ES, Elsherbiny ES. Ziziphus spina-christi (L.) fortified with Camellia sinensis mediates apoptosis, Notch-1 signaling, and mitigates obesity-induced non-alcoholic fatty liver. J Food Biochem 2021; 45(8): e13849. doi:10.1111/jfbc.13849.

[72] El Seedy GM, El-Shafey ES, Elsherbiny ES. Fortification of biscuit with sidr leaf and flaxseed mitigates immunosuppression and nephrotoxicity induced by cyclosporine A. J Food Biochem 2021;45(4):e13655.

[73] Viaud S, Saccheri F, Mignot G, Yamazaki T, Daillere R, Hannani D, et al. The intestinal microbiota modulates the anticancer immune effects of cyclophosphamide. Science 2013;342(6161):971–6. doi: https://doi.org/10.1126/science.1240537.

[74] Boursier J, Mueller O, Barret M, Machado M, Fizanne L, Araujo-Perez F, et al. The severity of nonalcoholic fatty liver disease is associated with gut dysbiosis and shift in the metabolic function of the gut microbiota. Hepatology 2016;63(3):764–75. doi: https://doi.org/10.1002/hep.28356.

[75] Bian X, Miao W, Zhao M, Zhao Y, Xiao Y, Li N, et al. Microbiota drive insoluble polysaccharides utilization via microbiome-metabolome interplay during Pu-erh tea fermentation. Food Chem 2022;377:. doi: https://doi.org/10.1016/j.foodchem.2021.132007132007.